Journal of Materials Chemistry C

ROYAL SOCIETY OF CHEMISTRY

REVIEW

View Article Online
View Journal | View Issue

Cite this: *J. Mater. Chem. C*, 2024, **12**, 11319

Unravelling the intricacies of solvents and sulfur sources in colloidal synthesis of metal sulfide semiconductor nanocrystals

Vincent Mauritz and Ryan W. Crisp *

Synthetic routes producing colloidal metal sulfide semiconductors vary in mechanism depending on the sulfur precursor utilized in the reaction. This review provides overarching insights into the molecular mechanisms underpinning successful material synthesis. The diverse range of sulfur precursors are categorized here into eight general classes representing the most common types of reagents: S_8, thioacetamide, thiols, thioethers, dithiocarbamates, carbon disulfide, thioureas, and trialkylphosphine sulfides. These precursors for non-aqueous synthesis provide reactive sulfur species *via* different pathways to form metal sulfides. The reaction pathways are discussed with a focus on creating quantum-confined colloidal nanocrystals, *i.e.* quantum dots (QDs), that are applicable as optoelectronic materials. This literature review underscores the nuanced interplay between sulfur source, reaction solvent, and reaction mechanisms, providing insights crucial for tailoring new metal sulfide synthesis strategies.

Received 5th April 2024,
Accepted 18th June 2024

DOI: 10.1039/d4tc01414f

rsc.li/materials-c

1. Introduction

The history of metal sulfide semiconductors dates back to 1833 when Michael Faraday discovered that the resistance of silver sulfide samples decreased when they were heated. Later, in 1874, Karl Ferdinand von Braun discovered rectification in metal sulfide samples.[1]

Both discoveries laid the groundwork for metal sulfide semiconductors and until today we try to investigate and understand the properties of these materials.

The use of these metal sulfide semiconductors varies from optoelectronics[2] over photocatalysis[3] to biology.[4] In optoelectronics and catalysis, the electronic structure of the active materials is of key importance. One parameter which is defined

Chemistry of Thin Film Materials, Friedrich-Alexander-Universität Erlangen-Nürnberg, Cauerstraße 3, 91058 Erlangen, Germany. E-mail: ryan.crisp@fau.de

Vincent Mauritz

Vincent Mauritz completed his MSc degree at the end of 2021 in Molecular Nanoscience at the Friedrich-Alexander-Universität (FAU) Erlangen-Nürnberg in Germany on the topic of size control of colloidal quantum dots (QDs) under the supervision of Ryan W. Crisp. In the same group, he started his doctoral research in Chemistry at the beginning of 2022 to further investigate organometallic synthesis of colloidal metal sulfide nanocrystals.

Ryan W. Crisp

Ryan W. Crisp studied Engineering Physics and Applied Physics at the Colorado School of Mines in Golden, Colorado for his BSc and MSc. He obtained his PhD in Applied Physics in 2015 after researching the optoelectronic properties, fabrication, and characterization of QDs and nanocrystals for solar cells with Joseph M. Luther at the National Renewable Energy Lab (NREL). He then went abroad to TU Delft as a postdoc with Arjan Houtepen on synthesis, spectroscopy, and charge carrier transport in QDs. Now he is working towards his habilitation at FAU with Julien Bachmann and leading his group to explore synthesis of new materials and developing new processes for application in photo-driven chemistry.

by the atoms in the crystal structure is the band gap and the position of the band gap against vacuum.[5] Comparing the band gaps of the chalcogenide main group from oxide to telluride, the average band gaps of the metal chalcogenides decrease.[6] This is because contributions to the valence band are by the chalcogen p-orbitals, which have higher energy going from 2p (oxygen) over 3p (sulfur) to 4p (selenium) and 5p (tellurium).[7] In this varying range of band gaps, metal sulfide materials fit well for optoelectronic and photocatalytic materials and often exhibit favourable phenomena like efficient multiple exciton generation[8–10] and other multicarrier effects as discussed in other reviews (see ref. 11). To further tune the properties within a material, scientists took advantage of a unique feature of nanomaterials, namely the confinement effect where electrical properties can change in a certain size regime that can be accessed synthetically.[12]

Nanomaterial synthesis can be done with a variety of approaches, including methods like chemical vapor deposition,[13] lithography,[14] or mechanical milling[15] or solution-based methods like solvothermal,[16] aqueous,[17] and organometallic-based synthesis.[18] Solution-based approaches exhibit the advantages of easy processability for later applications or in the simplicity of the required equipment.[19,20] In this review, we highlight the reaction mechanisms of common sulfur sources in the organometallic synthesis approach and their potential applications. In the colloidal synthesis, a dissolved metal precursor (*i.e.*, metal halide, metal oxide, organometallic precursor) is either combined with a sulfur source and heated (*i.e.*, heat-up synthesis) or one of the precursors in a solvent is rapidly injected at the reaction temperature into the other precursor-solvent mixture (*i.e.*, hot-injection synthesis). These approaches use long alkane chain solvents because of their high boiling points and chemical stability. Three classes of these solvents can be identified. First, long alkane chain amines, either saturated or partly unsaturated, like oleylamine (OLA) or *n*-hexadecylamine (HDA). Second, long alkane chain carboxylic acids, also saturated or partly unsaturated, like oleic acid (OA) or nonanoic acid. Third, long alkanes, either unsaturated or partly saturated like 1-octadecene (ODE) or squalene. Which of these solvents are selected depends on the requirements of each synthesis. In this review we investigate the reactions and also reaction mechanisms of common sulfur sources with common solvents used in this synthesis approach. For this we selected OLA as amine solvent, OA as a carboxylic acid solvent, and 1-octadecene. We found that for certain sulfur precursors the solvent plays a role in the reaction or decomposition mechanism with intermediate species formed and for others the sulfur source alone undergoes a decomposition mechanism. Understanding these reactions gives an intuition for metal sulfide syntheses and an understanding of which solvent and sulfur source is suitable.

2. Sulfur sources for colloidal metal sulfide nanocrystal synthesis

2.1. Sulfur

Elemental sulfur with its abundance in the earths' crust between 350 ppm and 697 ppm, depending on the definition used for the earths' crust, is ranked as the 13th to 16th most abundant element.[21–24] While sulfur exists in over thirty different allotropes, the most common allotropes have a crystalline phase consisting of rings with different sizes.[25] The typical allotrope is S_8, whereas this configuration is divided into three forms, namely α-S_8, β-S_8 and γ-S_8. It adopts a crown formation consisting of eight sulfur atoms and has its typical yellow colour.[26] The use of elemental sulfur in nanoparticle synthesis with long alkane chain solvents (OLA, ODE) dates back to the early 2000s, where elemental sulfur is typically dissolved in these solvents and then injected into a metal precursor solution to yield metal sulfide nanoparticles.[27–30] The reaction mechanism between primary amines and elemental sulfur was investigated in the 1960s by Davis and Nakshbendi.[31] In this mechanism, two primary amines react with the sulfur ring to yield an open chain alkylammonium *N*-polythioamine salt (Fig. 1a). A second reaction also occurs where the primary amine and the sulfur react to yield the respective thioamide and hydrogen sulfide, but the authors of this study state that this reaction occurs at a negligible rate at room temperature (Fig. 1b). These proposed reactions proceed at room temperature, which must be accounted for in contrast to the higher temperatures used in organometallic metal sulfide nanoparticle synthesis.[32–34] For a deeper understanding of the reaction between sulfur and amines at elevated temperatures, Thomson *et al.* investigated a solution of *n*-octylamine and elemental sulfur in different ratios *via* NMR.[35] By using 1D and 2D NMR techniques they were able to determine the byproducts of the reaction at room temperature, 80 °C, and 130 °C. At room temperature and 80 °C, which is the typical temperature of a sulfur amine solution prepared to inject in a metal sulfide synthesis, most of the sulfur exists in octylammonium polysulfides (Fig. 1c). The authors stated that it is unknown how the formation of these ammonium polysulfides work without the addition of any proton source (like H_2S). These results contrast with the mechanism postulated by Davis and Nakshbendi, though both postulate the ring opening of the sulfur and the reaction with the amine. The difference lies in the bonding nature of the sulfur. Davis and Nakhsbendi postulated a covalent bond between one sulfur atom of the sulfur chain and the nitrogen atom of the amine, while a negative charge on the other end of the sulfur chain and a positively charged ammonium ion form a salt like structure. Thomson *et al.* postulated that both sides of the opened sulfur chain are negatively charged and interact with positively charged ammonium ions. Increasing the reaction temperature to 130 °C for 2 h resulted in new species forming. The new species follow a chain reaction starting with the amine reacting with the polysulfide to form the respective thioamide under the release of hydrogen sulfide (Fig. 1d). Subsequently and similarly to reaction 1b, the thioamide reacts with another amine to *N*′-octyloctanamidine under the release of hydrogen sulfide (Fig. 1e). Then the *N*′-octyloctanamidine reacts with the polysulfide to form α-thioketoamidine (Fig. 1f). To the best of our knowledge, we could not find any mechanistic explanation for these reaction products in literature. As the authors suggest, this study should be a model for technical grade (70%) oleylamine. But oleylamine has a double bond at the 9th

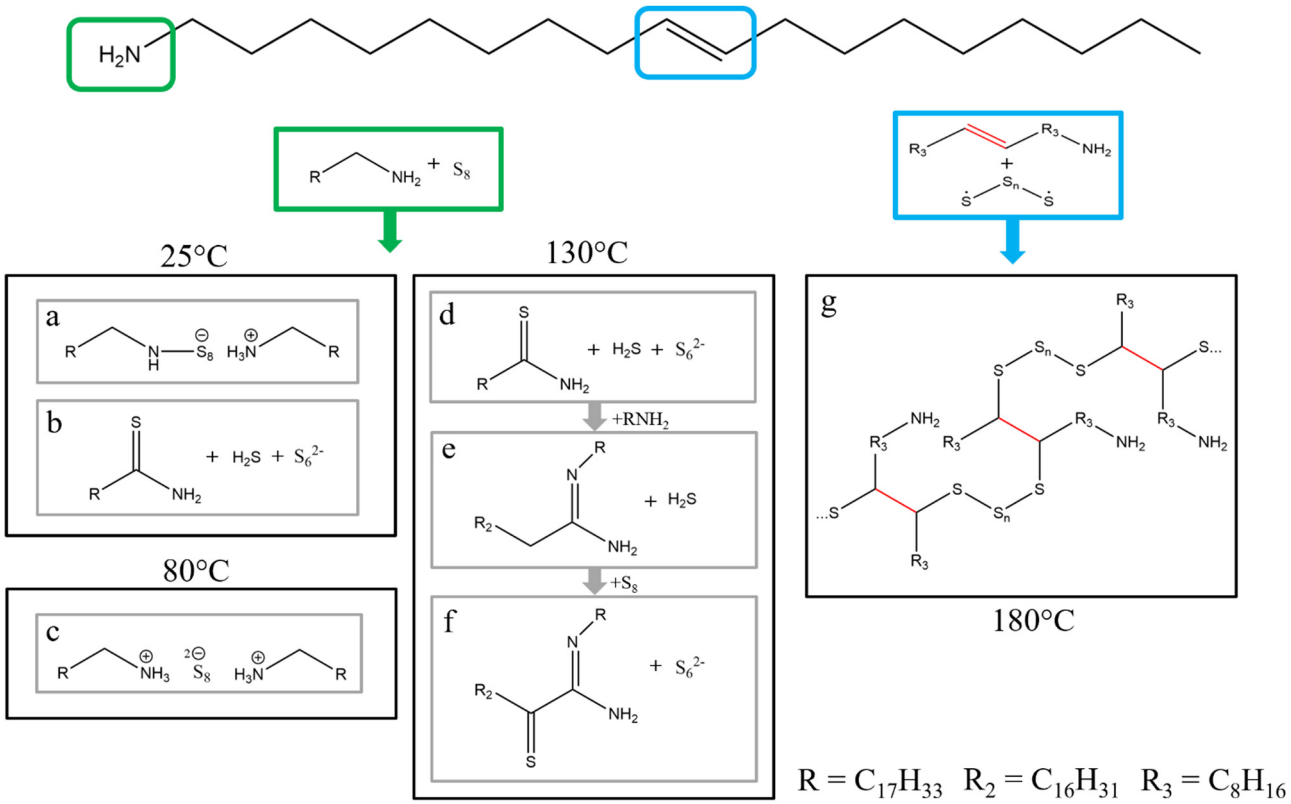

Fig. 1 Molecule structure for oleylamine. Depicted in the green box reaction of elemental sulfur with a primary amine functional group. (a) and (b) reaction at 25 °C reported in ref. 31 (c) reaction at 80 °C reported in ref. 35 (d)–(f) reaction at 130 °C reported in ref. 35. Depicted in the blue box reaction of elemental sulfur with the double bond in oleylamine. (g) polymerization reaction at 180 °C reported from ref. 36.

carbon position. This double bond is also reactive towards sulfur as suggested by Sahadevan *et al.*[36] Through a processes called "inverse vulcanization" they synthesized a sulfur–oleylamine copolymer (Fig. 1g).[36] To prepare this copolymer they melted sulfur (mp: 159 °C), which causes the S8 ring to open and form the sulfur diradical,[37,38] and added oleylamine. Stirring this solution at 180 °C for 8 minutes resulted in the copolymer. The crosslinking arises from the radical addition to the double bond of the oleylamine. Martin *et al.* even prepared a solution of a sulfur copolymer and used this copolymer as sulfur source and as coordinating ligand, in a cadmium sulfide nanoparticle synthesis, without the use of any additional solvent.[39] The copolymer was prepared by mixing melted sulfur with methylstyrene at 185 °C. In a solvent free synthesis, they combined the copolymer with cadmium acetate, resulting in cadmium sulfide nanoparticles.[39] Another approach to utilize the polymeric nature of sulfur is to apply it as a polysulfide metal complex for single-source precursors. Beal *et al.* synthesized zinc, iron, and nickel 1-methylimidazole polysulfide complexes.

The decomposition of these complexes at 300 °C led to metal sulfide nanocrystals with a variety of compositions and shapes.[40]

Another solvent to dissolve elemental sulfur is 1-octadecene.[41–43] With its double bond at the first carbon, it can react with the sulfur in two ways. First *via* a radical addition to the double bond or second *via* an ionic addition.[44,45] McPhail *et al.* studied the reaction between octadecene (technical grade) and elemental sulfur at 180 °C *via* NMR.[46] They identified three reaction products, sulfur added to the terminal carbon, sulfur added to the terminal carbon with the double bond moved to the beta carbon, and sulfur at the terminal carbon with branching on the beta carbon. Here again no mechanistic study was taken. Other literature suggests, as for the double bond in OLA, polymerization *via* a radical mechanism at the terminal double bond.[38,47]

Independent from the used solvent, elemental sulfur is used in nanoparticle synthesis in both a hot-injection[48–50] approach and a heat up[32,51,52] approach. The chemistry of the prepared sulfur–oleylamine mixture before injection at 80 °C can be partially explained by Thomson *et al.*[35] However, they neglected the double bond present in oleylamine. After injection, higher temperatures are used to grow nanoparticles, which raises a question about the actual reactive sulfur species since the temperatures used in the literature to describe most sulfur reactions do not exceed 180 °C (temperature comparisons are given in Section 2.9), but in the heat-up approach reaction temperatures often exceed 240 °C,[32,51,52] which means the reactive sulfur species remain unclear. The high number and complexity of the possible reactions of primary amines with sulfur makes it difficult to determine the actual reactive sulfur monomer species and at which temperature it is present.

In organometallic metal sulfide nanomaterial synthesis elemental sulfur is the first choice as sulfur source. But because of its different reaction pathways at different temperatures and

because it must be reduced to its S^{2-} state, it is not suitable for every organometallic metal sulfide nanoparticle synthesis if no reductive potential is present.

2.2. Thioacetamide

To circumvent the reduction of the sulfur source before the metal sulfide reaction, sulfur sources like thioacetamide are frequently used in nanoparticle synthesis.[53–55] In thioacetamide the sulfur comes as thione and already has the desired oxidation state of -II. It is a colourless crystal and is known to be carcinogenic.[56] Because of the slightly higher electronegativity of the sulfur (2.96)[57] and the higher electronegativity of the nitrogen (3.19)[57] from the amide group in contrast to the carbon, and the weak overlap of the 2p–3p–π bond,[58] its structure makes it affective for a nucleophilic addition at the thioketone carbon. Due to this mechanism, to the best of our knowledge, thioacetamide is used in two different synthesis approaches. First, hydrothermal synthesis where thioacetamide reacts with water to form *in situ* hydrogen sulfide and acetamide.[59,60] Hydrothermal routes would exceed the scope of this review and are therefore not included. The second synthesis approach is where thioacetamide is used with oleylamine as solvent. The general synthesis mechanism of primary amines and thioacetamide can follow three different paths as depicted in Fig. 2. The first reaction is a transamidation reaction of the amide group of thioacetamide with the release of ammonia. The second reaction is a nucleophilic substitution (SN_2) where the lone electron pair of the primary amine acts as nucleophile and substitutes the thione sulfur with the release of H_2S. The third possibility is simply the reaction of both the transamidation and the SN_2 reaction. All three reactions where proposed by Petroc and Andreev.[61] These reactions suggest that hydrogen sulfide is the reactive sulfur species. He *et al.* investigated the thioacetamide-oleylamine mixture at room temperature with FTIR. They found a weakening of the –C═S and –NH_2 vibrations and enhanced –C═N–, –C–N–, and –NH– vibrations, indicating the preferred formation of the both substituted product, which also concludes that hydrogen sulfide is the reactive sulfur species.[62]

Besides the reaction with oleylamine, Behera *et al.* suggested that thioacetamide acts as oxidizing agent in their synthesis. They studied the formation of $CuSbS_2$ nanoparticles with thioacetamide and sulfur as sulfur precursors. After the synthesis a second phase of $CuSbS_2$, namely Cu_3SbS_4, was found in the case for thioacetamide as sulfur source. In the second phase, antimony occurs in a higher oxidation state (+V), indicating a redox reaction during the synthesis. Since the higher oxidation state phase only occurred with thioacetamide as sulfur source they concluded that either the thioacetamide or acetonitrile, a decomposition product of thioacetamide, was reduced during the synthesis. To confirm the reduction they performed NMR studies on the reaction mixture and discovered a new methylene NMR resonance (different from the oleylamine methylene resonance) indicating the reduction reaction.[63] Since this oxidation should take place in every synthesis with oleylamine and thioacetamide, we searched through the literature to see if any other publication mentioned this reaction. We found that there is a clear trend in syntheses where researchers can use thioacetamide (Fig. 3). Thioacetamide thermally decomposes at 165 °C to acetonitrile and hydrogen sulfide.[64] Any nanoparticle reaction higher than the decomposition temperature of thioacetamide, resulted in either a partial oxidation of the used metal precursors or metal precursors in their already most stable oxidation state were used, resulting in materials with the most stable oxidation states, including Bi_2S_3,[65] Cu_2ZnSnS_4,[66] $Cu_{12}Sb_4S_{13}$,[67] NiS_2,[68] Cu_3SbS_4,[63] and SnS_2.[69] Syntheses proceeded at a lower temperatures, resulted in materials with not the most stable oxidation states like Cu(I) in $CuInS_2$ and Sn(II) in SnS.[53,70] Since the thioacetamide decomposition temperature clearly draws a line between those materials, the oxidative species can be assigned to the decomposition product acetonitrile. This trend confirms the finding of Behera *et al.*[63] and also gives an overview of when to use thioacetamide in nanoparticles synthesis, *e.g.* to synthesize particles with metals in less stable oxidation states.

2.3. Thiols

Thiols are another class of sulfur precursors used in nanoparticle synthesis.[71] Thiols have a sulfur-hydrogen bond as functional group. Since the electronegativity for hydrogen and sulfur are nearly the same (2.59 and 2.96,[57] respectively) the bonding is not as strong as in the corresponding alcohols, making thiols more acidic.[72] Thiols are considered a soft base

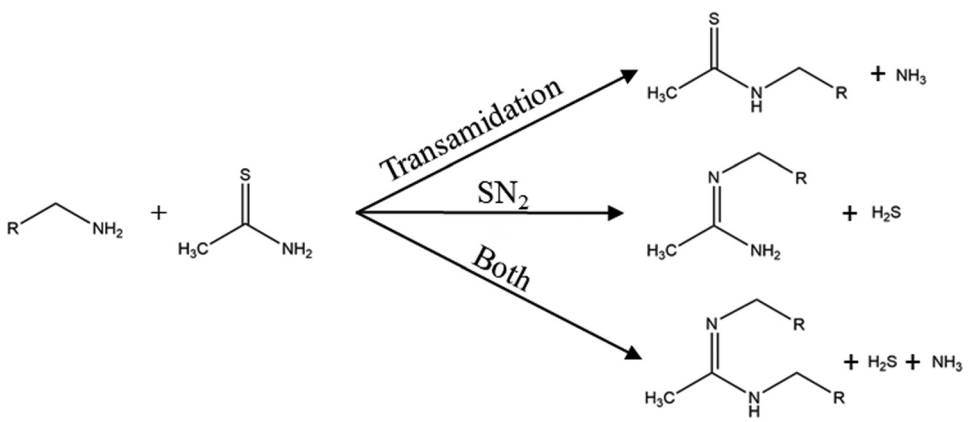

Fig. 2 Reactions of a primary amine with thioacetamide. Adapted with permission from ref. 61. Copyright 1971 IOP.

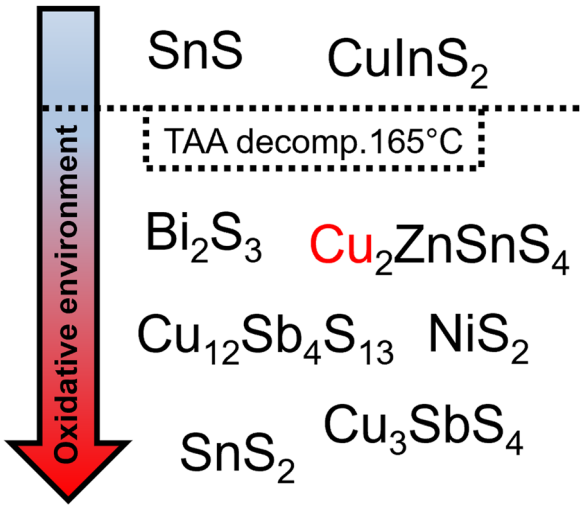

Fig. 3 Scheme of synthesized materials with thioacetamide (TAA) as sulfur source and oleylamine as solvent. Materials synthesized at higher temperatures as the decomposition temperature of TAA (165 °C) have the most stable oxidation state. Copper in Cu_2ZnSnS_4 (CZTS) is stated in red because Cu(I) is not the most stable oxidation state, but in the synthesis of CZTS Cu(II) is used as precursor, whereas Sn has its most stable oxidation state (+IV). Materials synthesized at lower temperature than the decomposition temperature of TAA can have an oxidation state different than the most stable one.

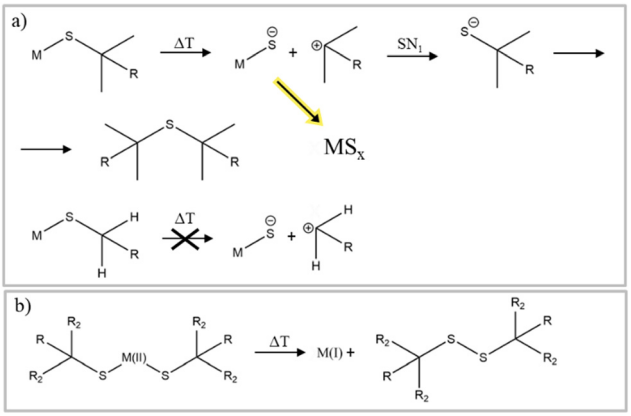

Fig. 4 (a) Thermal decomposition of thiols and formation of MS_x nanomaterials. Figure adapted from ref. 79 under Creative Commons Attribution licence CC BY 4.0 (b) redox reaction of thiols and metals reported in ref. 86.

in the hard and soft acids and bases (HSAB) concept and can form complexes with soft acid metals.[73] The most used thiols in nanoparticle synthesis are 1-dodecanethiol (DDT) and *tert*-dodecanethiol.[74–78] While 1-dodecanethiol has 12 carbons linearly attached to its thiol group, *tert*-dodecanethiol has also 12 carbons but the alpha carbon is ternary. The long alkane chain in both thiols gives them high boiling points, which makes them also good candidates for solvents and good surface ligands in nanoparticle synthesis.

For use only as sulfur source, thermal decomposition of the thiol compounds describes the reactive sulfur species. For *tert*-dodecanethiol Heo *et al.* synthesized metal thiolate compounds with *tert*-dodecanethiol and investigated the decomposition with mass spectrometry and Raman spectroscopy.[79] Thermal decomposition of metal thiolate precursors is depicted in Fig. 4a. First, thermal induced breaking of the carbon sulfur bond leads to a carbocation and a metal sulfide anion. Subsequently, the carbocation undergoes an SN_1 reaction with a thiolate anion to yield a dialkyl sulfide, while the remaining metal sulfide anions can grow into metal sulfide nanomaterials. This reaction mechanism indicates that the reactive sulfur species is already the thiol or rather the metal thiolate (complexes). The tertiary carbon, in *tert*-dodecanethiol, at α position stabilizes the carbocation, whereas for 1-dodecanethiol the primary carbon is unlikely to form carbocations, meaning that the same reaction mechanism cannot explain the decomposition of 1-dodecanethiol.[80] The use of copper(II) precursors for nanoparticle synthesis with the desired copper material in oxidation state +I like Cu_2S and CZTS is quite common, without any explanation about the reduction of the precursor.[74,81,82]

In other material systems like the indium pnictides (InP, InAs, InSb), a redox reaction where the pnictogen changes oxidation state has been more thoroughly investigated and found to aid in nanocrystal formation.[83–85] Norby *et al.* investigated the formation of Cu_2S nanoparticles with the use of Cu(II) acetate and DDT and the reaction *via* NMR. They suggested that the reduction of copper must involve the oxidation of another species in the reaction. Since only DDT was used as other reactant, it was confirmed *via* NMR that DDT was oxidized to didodecyl disulfide (Fig. 4b).[86] The copper(I) reacted with the excess DDT, to form a copper thiolate complex. The actual decomposition mechanism of DDT or the respective metal thiolates is not described in literature and referred to as carbon sulfur bond thermolysis or DDT decomposition.[87,88] Not only long alkyl thiols can be used as sulfur source. Thiols with different end groups like allyl, aryl, phenyl, short alkyl and also disulfides can be used. Rhodes *et al.*[89] used precursors from the above-mentioned classes (Fig. 5a) and investigated the reactivity and formation of iron sulfide colloids. They found that the lower the carbon sulfur bond dissociation energy is, the more sulfur-rich phases were obtained.[89] It was also outlined, as before, that the carbon–sulfur bond dissociation is dependent on the resonance stabilization of the carbocation. It can be stabilized with allyl and phenyl groups but not with alkyl groups.

As mentioned before alkyl thiols also can be used as ligands. If used directly in the synthesis, the sulfur of the thiol will be directly bound into the crystal structure (Fig. 5b), having the alkane chain sticking out of the crystal surface and acting as ligand, enhancing the stability of the colloidal nanocrystals, but makes them also resistant against ligand exchange procedures.[90] Alternatively, if introduced after the synthesis DDT can be used as ligand by a ligand exchange procedure and then bound to the surface as a X-type ligand.[91]

The versatile behaviour of thiols in metal sulfide nanomaterial synthesis either only as sulfide source or as solvent or ligand exhibits a huge potential for thiols. The first consideration about the use of thiols is the processability after synthesis.

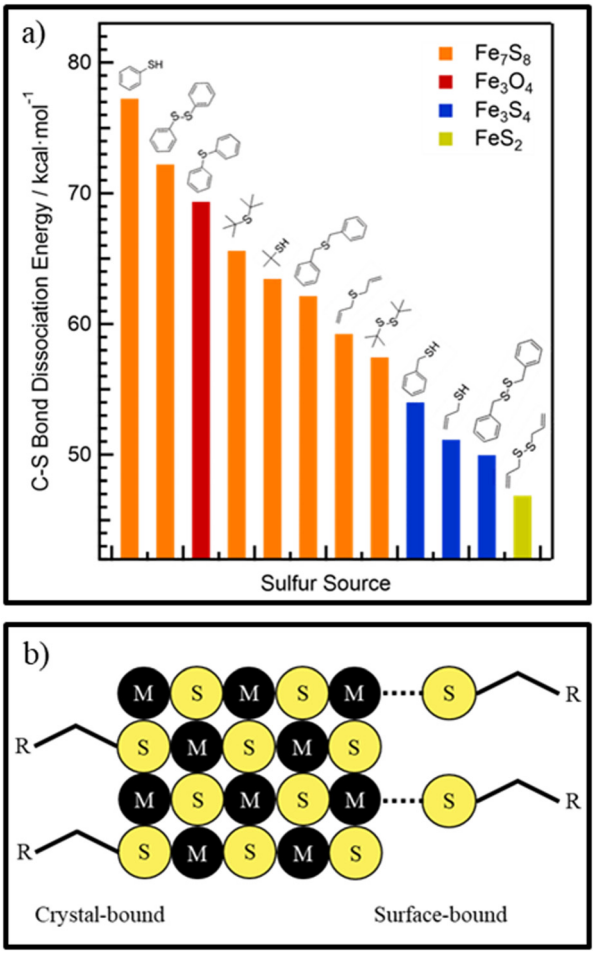

Fig. 5 (a) Reactivity of different sulfur precursors *vs.* the carbon–sulfur dissociation energy and their products in iron sulfide synthesis. Adapted with permission from ref. 89. Copyright 2017 American Chemistry Society. (b) Schematic picture of crystal-bound and surface-bound thiols. Adapted with permission from ref. 90. Copyright 2014 American Chemistry Society.

Because of the possibility of crystal-bound thiols, processing of these nanomaterials, for instance, ligand exchange procedures to smaller ligands for enhancing electrical conductivity or annealing procedures to fuse the nanomaterials, is difficult.[92] On the other hand, these crystal-bound ligands increase colloidal stability over longer times. Another consideration should be the R-group (*e.g.* an alkyl, aryl, *etc.*) of the thiol. The resulting C–S bond dissociation energy for different R-groups affects the formation kinetics of the nanocrystal.[89] The last consideration should be about the reductive potential of thiols. Suitable metal precursors should be chosen to avoid their reduction and the formation of undesired side products.[86]

2.4. Thioether: bis(trimethylsilyl)sulfide (TMS-S)

TMS-S, a liquid thioether, is used in nanoparticle synthesis because of its high reactivity and therefore the mild reaction temperatures (below 150 °C).[93–95] Its high reactivity results from the high affinity of silicon to oxygen or halides, releasing the sulfide anion.[96] Drawbacks of this affinity are the sensitivity to oxygen and moisture in the air, which makes it difficult to handle, and the strong odour. Also because of its high reactivity TMS-S is only used in hot injection synthesis, either as pure chemical or dissolved in ODE.[97–99] Literature using TMS-S as the active sulfur source dates back to the early 1990s,[100] and received more attention in the beginning of the 2000s.[99] But still up until now no detailed decomposition or reaction mechanism of TMS-S into metal sulfide nanomaterials is reported. The general reaction pathway follows the use of metal oxides[101] (or similar precursors with a metal oxygen bond *i.e.*, carboxylates) or halides[102] as precursors. Mixing the metal oxide with oleic acid leads to the formation of a metal carboxylate which then reacts with the TMS-S to form the respective metal sulfide and TMS-carboxylate. Metal halides mixed with OLA form a soluble metal amine complex[103] and, when TMS-S is injected, leads to an anion exchange and subsequently to metal sulfide nanomaterials. The reactivity of TMS-S allows for using metal precursors that have a metal-oxygen bond that would perhaps be too strong for other sulfur precursors to break. Anantovich *et al.* investigated the formation of PbS nanocrystals *via* the reaction of lead oleate and TMS-S in octadecene at mild reaction conditions.[104] At temperatures as low as 50 °C a complex of lead and bis(trimethylsilyl)sulfide results without the formation of PbS. Addition of a protic solvent like ethanol or water or an aprotic solvent like acetone resulted in the formation of PbS nanoparticles. For the addition of protic solvents two different reactions were proposed. The first one promotes the scission of the Pb–S bond resulting in the coordination of the alkoxide to the lead and the formation of trimethylsilylthiol, which subsequently form PbS nanoparticles. The second reaction involves the scission of the Si–S bond and the formation of the trimethylsilylester and coordinated thiol groups at the lead, again subsequently forming PbS nanoparticles. The reaction with the aprotic acetone resulted in the formation of thioacetone, which reacts to form PbS.

TMS-S in organometallic metal sulfide nanomaterial synthesis can be used for mild reaction conditions. The downside of this high reactivity is the difficulty to handle TMS-S in the laboratory. It must be kept air-free and it exhibits a strong unpleasant smell even at minimal concentration.

2.5. Dithiocarbamates

Dithiocarbamates (DTC) are the sulfur analogue to the carbamate functional group. Because of its possibility to coordinate a wide range of elements and a wide range of oxidation states and the easily changeable backbone, DTC are widely used in inorganic chemistry.[105–107] In nanoparticle synthesis DTC are used as single source precursors for secondary, ternary and quaternary transition metal sulfides together with a primary amine like OLA as solvent.[108–110] Since DTC are used as single source precursors the decomposition occurs intramolecular leaving metal sulfide monomers, which then can form metal sulfide nanomaterials. In this decomposition, the solvent, a primary amine is involved in the decomposition reaction and significantly lowers the decomposition activation energy.[111] Depending on the oxidation state of the coordinated metal centre and its other possible oxidation states, different decomposition routes are possible. Fig. 6 is divided into four parts indicated by the coloured boxes. Starting with a metal centre in +III oxidation state, as depicted in the

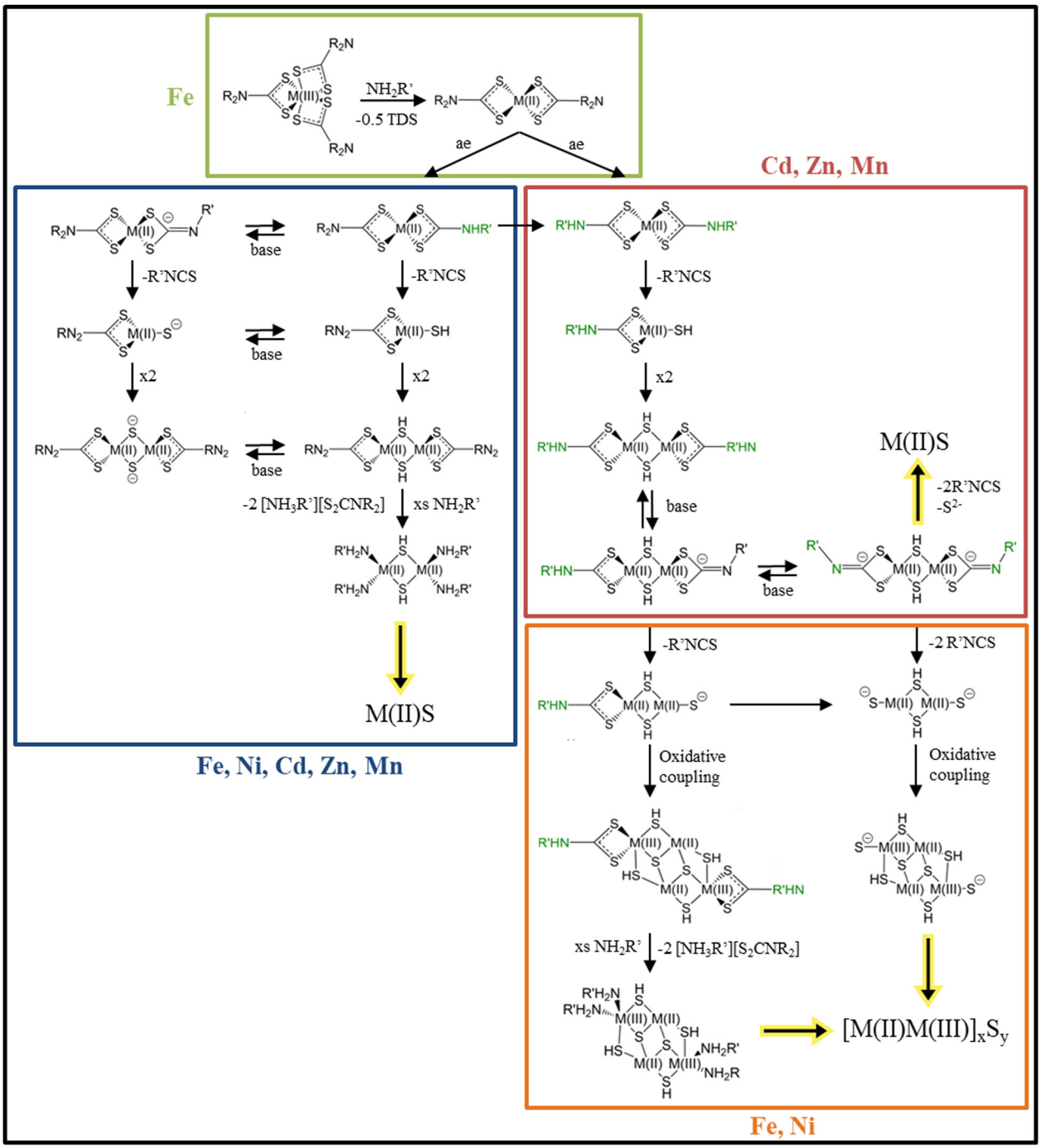

Fig. 6 Possible reactions of metal dithiocarbamate complexes in a primary amine solvent. Summarized reactions from ref. 111–113, 115 and 116. For simplicity the possible coordinated primary amine molecules are left out.

green box, three DTC moieties are coordinated to the metal centre. In a solution of oleylamine or general a primary amine this metal centre gets thermally reduced by electron transfer from the +III metal centre to one DTC to the +II oxidation state, leaving the metal centre with two coordinated DTC molecules and the elimination of thiuram disulfide (TDS).[112] This is the case when iron +III is used in combination with DTC and oleylamine. Going from the two coordinated +II metal centre (green box) two reactions can happen. The primary amine can either exchange one amido backbone (amido exchange = ae), as pictured in the blue box *via* a proton transfer or both backbones (red box), depending on the reaction temperature and the used primary amine. If just one backbone is exchanged as depicted in the blue box, a subsequent proton transfer from the exchanged amido group to one of the sulfurs coordinated to the metal centre, leads to the elimination of an isothiocyanate and leaving the metal

centre with a bound thiol. Two of these molecules dimerize *via* the thiol groups, followed by the loss of the DTC moieties, leaving amine-coordinated, thiol-bridged, MS units that further grow into nanocrystals. Further decomposition results in metal(II) sulfide nanomaterials. Since primary amines like OLA have a low pK_B value (3.3)[113] all the before mentioned reactions can happen *via* the deprotonated species as indicated by the base equilibrium arrows. In literature this reaction is thought to happen for metals in +II state like Fe, Ni, Cd, Zn, and Mn.[111,112,114–116] If both backbones of DTC are amido exchanged, as shown in the red box, also a proton transfer from the amido backbone to one of the sulfurs of DTC happen and subsequent elimination of isothiocyanate. Dimerization results in two metal centres with thiol bridges. In basic conditions, the amido proton is eliminated (both sides) and two isothiocyanate moieties and a sulfide are eliminated, leading to the formation of M(II)S nanomaterials. This decomposition process is thought to happen for elements in +II state like Cd, Zn, Mn.[111,112,114–116] Hollingsworth *et al.* investigated the differences in nickel(II) dithiocarbamate decomposition for two different primary amines, OLA and *n*-hexylamine, experimentally and theoretically.[111] *Via* density functional theory (DTF) calculations they found that the exchange process proceeds *via* a proton transfer from the primary amine to the amide in a metathesis-like four membered transition state. Because the amide exchange rate of OLA is slower than the rate of *n*-hexylamine, a mixture of both NiS and Ni_3S_4 resulted, while with *n*-hexylamine only NiS resulted. These results indicate a fourth decomposition route (orange box) since parts of the nickel were oxidized to Ni_3S_4. Starting from the double exchanged, amido deprotonated, and thiol bridged molecule, elimination of an isothiocyanate leads to negative charged sulfides at the metal centres. Subsequent oxidative coupling of two of these molecules results in an oxidation state mixture of the metal (+II and +III), leading to a mixed metal sulfide.[111,112] Further confirming this decomposition mechanism, Dirksen *et al.* found that mixing zinc DTC complexes with primary amines resulted in the formation of different substituted thioureas, formed *via* a nucleophilic attack of the primary amine with the isothiocyanate.[117]

The ability to bind to a variety of metals and the versatility to exchange the backbone the DTC and therefore to tune the kinetics of the decomposition opens a wide range of usability. But because of the secondary oxidative reaction pathway, metal precursors must be chosen appropriately to prevent any unwanted secondary phases appearing during the synthesis.

2.6. Carbon disulfide

Similarly, to TMS-S, CS_2 comes in liquid form and is difficult to handle because of its low boiling point of 46.3 °C[118] and its toxicity.[119] The two sulfur atoms are bound to one carbon atom *via* a double bond (thione). Ahmad *et al.* studied the formation of CZTS with CS_2 as sulfur source in OLA.[120] They also studied the reaction between CS_2 and OLA in anisole *via* NMR. In this reaction, two moieties of oleylamine react with CS_2, where the lone pair of the OLA acts as nucleophile and attacks the electrophilic carbon in CS_2, to form an oleyldithiocarbamate anion with an oleylammonium as counter ion (Fig. 7a). Subsequent decomposition of the oleyldithiocarbamate into metal sulfide nanomaterials should follow the decomposition route of dithiocarbamates discussed in the previous section. As in the last example CS_2 only acts as intermediate precursor for the active sulfur species. In literature a second reaction of CS_2 and primary amines is described. Ballabeni *et al.* synthesizes thioureas with primary amines and CS_2.[121] In this reaction the amines and CS_2 react to a carbamodithioic acid which then reacts to a isothiocyanate and H_2S. Subsequently, with another moiety of an amine the isothiocyanate reacts to form a thiourea. While the first reaction yields an oleyldithiocarbamate which will coordinate the used metal ions and then decompose to also form olelyisthiocyanate and sulfur bound to metal, the second reaction directly produces hydrogen sulfide which then can react with the metal(s) (Fig. 7b). Both reactions initially started with the same reaction stop, forming a dithiocarbamate. But while reaction (a) exhibits the deprotonated form, stabilized by the used solvent, reaction (b) continues to react because of the protonated dithiocarbamate form. Additional differences in the reactions are the use of shorter carbon chain primary amines (longest chain has 8 carbons) and the use of a catalyst by Ballabeni *et al.*[121]

Since CS_2 decomposes into dithiocarbmate, the same consideration as discussed in the section of DTCs must be made. Additionally, because of its low boiling point, CS_2 can be difficult to handle in the laboratory.

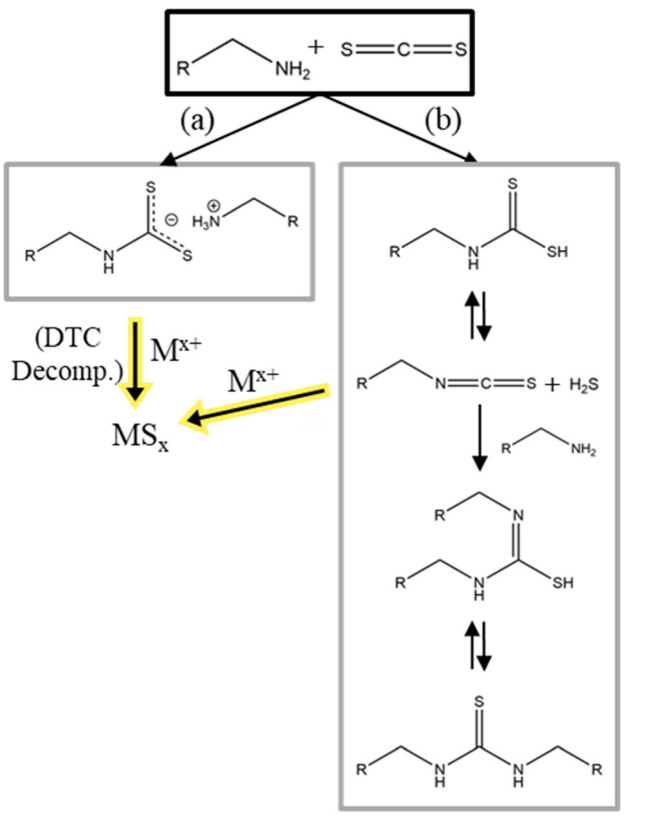

Fig. 7 Reactions of carbon disulfide with a primary amine and decomposition reaction into the corresponding metal sulfides. (a) reaction reported in ref. 120 (b) reaction reported in ref. 121.

2.7. Thioureas

Thioureas can be divided into two different classes, substituted thioureas and thiourea. In this class of molecules, sulfur exists as thione with amide groups bound at both sides of the thione. Both thiourea classes find use in a variety of metal sulfide nanoparticles syntheses.[122–124] Depending on the substitute, the reaction rate and therefore the resulting nanomaterial product and product properties such as shape, size, *etc.* can be tuned. Hendricks *et al.* prepared a library of symmetric and asymmetric substituted thioureas and investigated their reactivity as sulfur source in lead sulfide nanocrystal synthesis.[125] The different reaction rates of the thioureas lead to control over the size of the nanoparticles. Looking at the formation of metal sulfide nanocrystals and the decomposition of thioureas, substituted thioureas and thiourea have to be analysed individually. The decomposition of thiourea is described in two ways.

First, thiourea can be used as complexing agent. Depending on the metal and on the substituents, it can complex either with the sulfur[126] or with the sulfur and one nitrogen of the amide group (only for substituted thioureas).[127] Introducing a metal salt to a solution of thiourea and subsequent heating leads first to the formation of these complexes and then to the decomposition to metal sulfide nanomaterials (Fig. 8a).[128,129] There is nothing experimentally reported about the byproducts of this metal thiourea complex decomposition but it is thought that it decomposes in cyanamide which then is likely to trimerize to melamine.[130] Second, mixing a thiourea solution with a metal carboxylate leads to the dimerization to ammonium thiocyanate because of the driving force of the carboxylate to coordinate the ammonium ion. Subsequently, they react to form an amide and the gases carbonyl sulfide and ammonia. The metal ions simultaneously react with the isothiocyanate ion to form a complex which then can decompose to a metal sulfide (Fig. 8b). Since a part of the thiocyanate reacts with the carboxylate and the other part with the metal the resulting metal sulfide can exhibit a sulfur deficiency as Shults *et al.* reported in their metal sulfide synthesis.[128]

Substituted thioureas follow a different decomposition pathway. There is an equilibrium between substituted thioureas and isothiocyanates plus primary amines, depending on the temperature (Fig. 9).[131] If the equilibrium is on the side of the thiourea, the added metal precursor can coordinate to the sulfur of the thiourea and then decompose to the desired metal sulfide. The thiourea decomposes into a carbodiimide, which can further react with a primary amine to a guanidine, as depicted in Fig. 9a.[132] If the equilibrium is one the isothiocyanate side and a metal carboxylate is added the reaction proceeds *via* a cyclic rearrangement which results in the respective amide and carbonyl sulfide.[133] This carbonyl sulfide can react with the metal ions and decompose to form metal sulfide nanomaterials (Fig. 9b).[134]

As for thiols and dithiocarbamates, the exchangeable backbone of substituted thioureas can tune the reaction kinetics and therefore exhibits a diverse usability.

2.8. Trialkylphosphine sulfides

Trioctylphosphine sulfide (TOP-S) or the general group of phosphine sulfide are characterized by the phosphorus sulfur double bond and three bound rests, mostly alkane chains, whereas the reactivity of the P=S bond depends on the specific R-groups.[135] The use of TOP-S in nanomaterial synthesis is well reported in literature,[136,137] but to the best of our knowledge only one mechanistic reaction study of phosphine sulfide to metal sulfide nanoparticles is reported. In this study from Liu *et al.* the metal carboxylate precursor is thought to coordinate through the metal to the sulfur of the phosphine sulfide.[138] This activates the phosphorus-sulfur bond and subsequent nucleophilic attack from a metal precursor anion leads to elimination of metal sulfide and the bonding of the carboxylate to the phosphorus. The bound carboxylate undergoes another reaction with another carboxylate molecule to form the carboxylate anhydride and trioctylphosphine oxide. A further property of TOP-S is the use in a chalcogenide anion exchange procedures for already synthesized nanomaterials. Mahadevu *et al.* synthesized lead oxide nanocrystals and let them react with TOP-S at room temperature over several hours.[139] A complete anion exchange from oxygen to sulfur could be observed. TOP-S can even be used as sulfur source for facet selective growth in core shell nanomaterials structures as investigated by

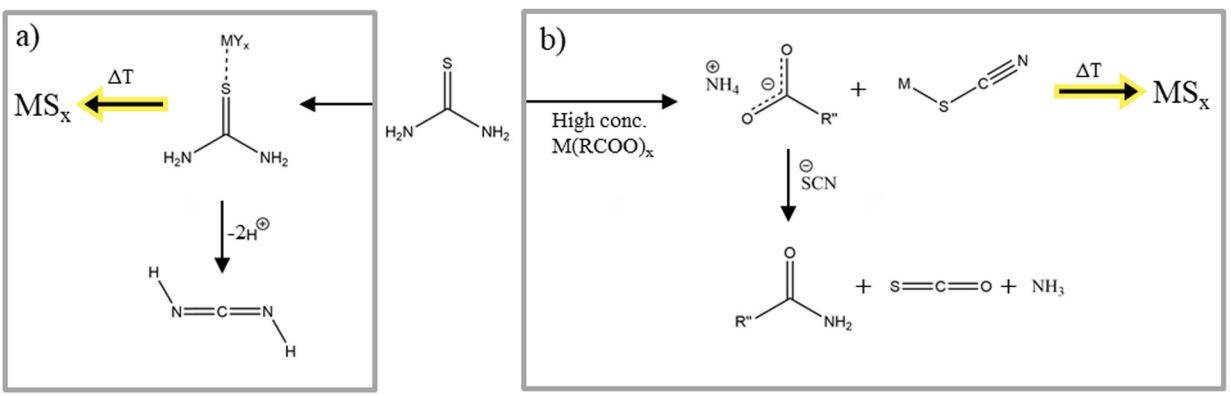

Fig. 8 (a) Decomposition reaction of thiourea into metals sulfides, (b) decomposition reaction of thiourea with metal carboxylates into metal sulfide materials. Figure adapted from ref. 128 under Creative Commons Attribution licence CC BC 4.0.

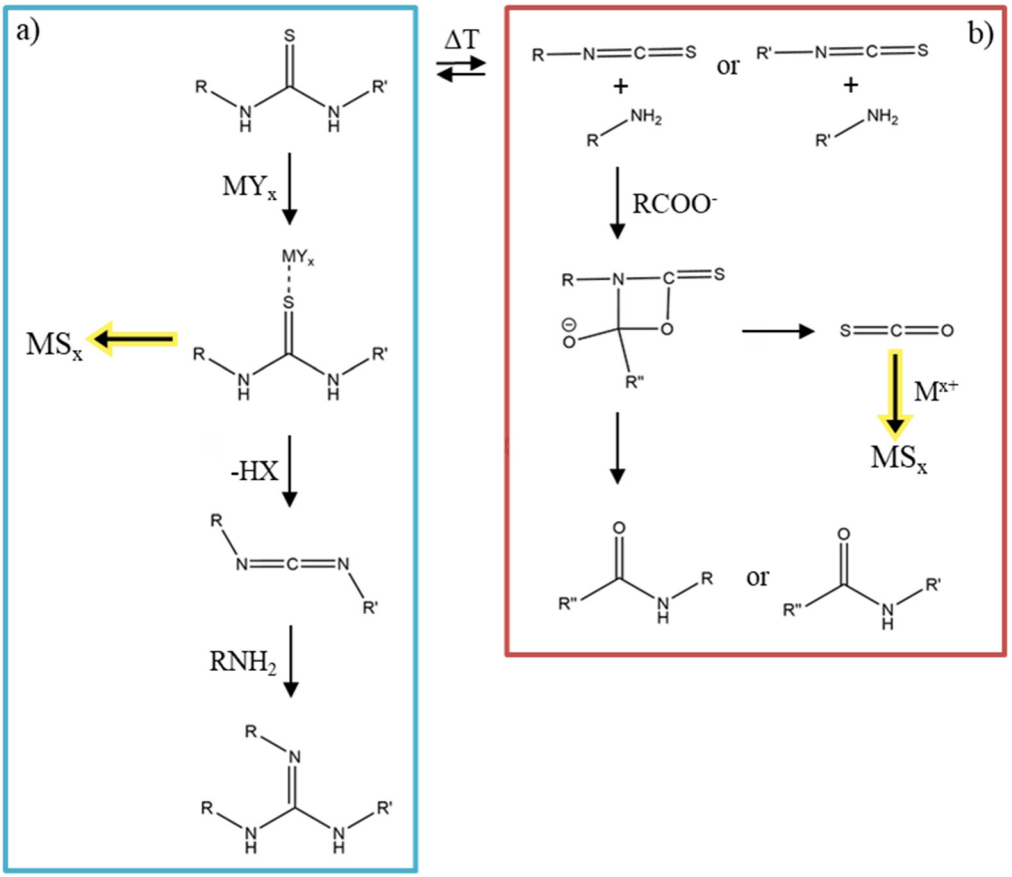

Fig. 9 (a) The decomposition reaction of substituted thioureas into metal sulfides. Adapted with permission from ref. 132. Copyright 2023 American Chemistry Society. (b) The decomposition reaction into metal sulfides from thioureas at higher temperatures with equilibrium on the isothiocyanate side. Figure adapted from Ref. 133 and 134.

Fan *et al.*[140] The authors used TOP-S to selectively grow a CdS shell around a CdSe core.

2.9. Conclusion and summary

Table 1 gives information about the temperatures the sulfur sources were used for synthesis and indication about the handling. A big influence on the reaction does not only have the sulfur source or the solvent, also the choice of the metal precursor must also be considered. Further reviewing of these papers should give a better understanding for the metal precursor choice.[141,142]

3. Future directions

In this review, we summarized the reactions and reaction mechanisms of different sulfur sources in the organometallic nanomaterials' synthesis approach. These sulfur sources have sulfur bound in different configurations and therefore the reactivity and reaction intermediaries are different. This behaviour can influence the general choice of precursor and reaction parameters for a successful organometallic nanomaterial synthesis. Not only the sulfur configuration influences the choice of precursor but also several other categories influence the reaction behaviour. The first category is the reaction

Table 1 Sulfur sources and reaction temperatures used in literature along with notes on their specific handling

Sulfur source	Temperature [°C] (ref.)	Handling
Elemental Sulfur	280 ([27]), 320 ([27]), 220 ([27]), 140 ([28]), 300 ([29]), 120 ([143])	Yellow crystalline solid with easy handling
Thioacetamide	130 ([53]), 230 ([53]), 50 ([54]), 160 ([55]), 200 ([55])	Colourless solid with toxic and carcinogenic properties
Thiols	240 ([74]), 260 ([81]), 220 ([89]), 280 ([86])	Properties differ but mostly used in liquid form
Bis(trimethylsilyl)sulfide	60 ([93]), 120 ([94]), 130 ([94]), 120 ([95]), 90 ([101])	Strong smelling liquid with toxic properties
Dithiocarbamates	230 ([108]), 260 ([108]), 280 ([108]), 230 ([114]), 180 ([115]), 270 ([115]), 250 ([116])	Properties differ but mostly used in solid form
Carbondisulfide	200 ([120])	Liquid with low boiling point and toxic properties
Thioureas	280 ([122]), 250 ([122]), 240 ([123]), 90 ([125]), 150 ([125]), 210 ([128]), 220 ([128]), 360 ([144])	Properties differ bust mostly used in solid form
Trialkylphosphines	300 ([136]), 250 ([137]), 25 ([139])	Properties differ but mostly used in liquid form

pathway to the point when the reactive sulfur species is produced. Many of these sulfur sources need more than one reaction step to reach the reactive sulfur species. This opens the possibility of many side products which can or will influence the whole reaction. This is dependent on precursor concentration and temperature leading to fluctuations in reproducibility and variations in the product. Only three sulfur precursors need one reaction step to yield the reactive sulfur species namely thioacetamide, thiourea, and (trimethylsilyl)sulfide. The second category is the ease of exchanging the carbon backbone or the other constituents of the sulfur source which offers the possibility to tune the decomposition kinetics of the sulfur source and thus the kinetics of the whole reaction, influencing the properties of the resulting nanomaterials like size, shape, and/or electrical/optical properties. Commercially available or self-made thiols, dithiocarbamates, and substituted thioureas have been investigated in this regard. The third category addresses the redox potential of some of the sulfur sources. As mentioned before several reaction steps until the reactive sulfur species is available can lead to unwanted side products. These side products can also lead to redox reactions in the reaction medium. Thioacetamide and dithiocarbamates and their respective side products can create an oxidative environment leading to oxidation of some of the metal precursor and therefore to unwanted reaction products or phases. On the other hand, thiols exhibit the potential to create a reductive environment reducing the used metal precursor. The final category is safe handling. Crystalline precursors like elemental sulfur, thioacetamide, dithiocarbamates, and thioureas can be handled with simpler safety precautions. However, these crystalline solids can exhibit hygroscopic properties influencing their properties in the reaction. Oily liquids like thiols and trialkylphosphines (depending on the chain length) can also be processed easily with routine safety precautions. Reactive liquids with high vapor pressure like carbon disulfide and (trimethylsilyl)sulfide should be handled with great caution and safety measures to prevent exposure to personnel. When planning an organometallic metal sulfide synthesis with oleylamine, oleic acid, or 1-octadecene all these categories should be considered and analysed.

While metal sulfide synthesis has been researched for over a century, there are still gaps in the literature, as discussed. An in-depth explanation of the reaction or reaction mechanism for these precursors in conjunction with the various metal sources is still needed to deeply understand and further fine tune their properties.

Author contributions

The manuscript was written through contributions of both authors.

Data availability

No primary research results, software or code have been included and no new data were generated or analysed as part of this review.

Conflicts of interest

There are no conflicts to declare.

Acknowledgements

This work is funded by the Deutsche Forschungsgemeinschaft (DFG) – Project number 465220299.

References

1 P. R. Morris, *A History of the World Semiconductor Industry*, 1990.
2 Y. Li, A. A. Murthy, J. G. DiStefano, H. J. Jung, S. Hao, C. J. Villa, C. Wolverton, X. Chen and V. P. Dravid, MoS_2-capped CuxS nanocrystals: a new heterostructured geometry of transition metal dichalcogenides for broadband optoelectronics, *Mater. Horiz.*, 2019, **6**, 587–594.
3 H. Hao and X. Lang, Metal Sulfide Photocatalysis: Visible-Light-Induced Organic Transformations, *ChemCatChem*, 2019, **11**, 1378–1393.
4 E. R. Donati and W. Sand, *Microbial Processing of Metal Sulfides*, Springer, 2007.
5 R. Woods-Robinson, Y. Han, H. Zhang, T. Ablekim, I. Khan, K. A. Persson and A. Zakutayev, Wide Band Gap Chalcogenide Semiconductors, *Chem. Rev.*, 2020, **120**, 4007–4055.
6 D. Xia, Q. Chen, Z. Li, M. Luo and P. K. Wong, in *Chalcogenide-Based Nanomaterials as Photocatalysts*, ed. M. M. Khan, Elsevier, 2021, pp. 135–172, DOI: 10.1016/B978-0-12-820498-6.00006-8.
7 Y. Xia and J. Yu, *Semiconductor Solar Photocatalysts*, 2021, pp. 299–324, DOI: 10.1002/9783527834327.ch4c.
8 F. C. M. Spoor, G. Grimaldi, C. Delerue, W. H. Evers, R. W. Crisp, P. Geiregat, Z. Hens, A. J. Houtepen and L. D. A. Siebbeles, Asymmetric Optical Transitions Determine the Onset of Carrier Multiplication in Lead Chalcogenide Quantum Confined and Bulk Crystals, *ACS Nano*, 2018, **12**, 4796–4802.
9 Y. Yan, R. W. Crisp, J. Gu, B. D. Chernomordik, G. F. Pach, A. R. Marshall, J. A. Turner and M. C. Beard, Multiple exciton generation for photoelectrochemical hydrogen evolution reactions with quantum yields exceeding 100%, *Nat. Energy*, 2017, **2**, 17052.
10 D. M. Kroupa, G. F. Pach, M. Vörös, F. Giberti, B. D. Chernomordik, R. W. Crisp, A. J. Nozik, J. C. Johnson, R. Singh, V. I. Klimov, G. Galli and M. C. Beard, Enhanced Multiple Exciton Generation in PbS|CdS Janus-Like Heterostructured Nanocrystals, *ACS Nano*, 2018, **12**, 10084–10094.
11 C. Melnychuk and P. Guyot-Sionnest, Multicarrier Dynamics in Quantum Dots, *Chem. Rev.*, 2021, **121**, 2325–2372.
12 E. Roduner, Size matters: why nanomaterials are different, *Chem. Soc. Rev.*, 2006, **35**, 583–592.
13 F. Makin, F. Alam, M. A. Buckingham and D. J. Lewis, Synthesis of ternary copper antimony sulfide via solventless thermolysis or aerosol assisted chemical vapour deposition using metal dithiocarbamates, *Sci. Rep.*, 2022, **12**, 5627.

14 Y. Wang, J.-A. Pan, H. Wu and D. V. Talapin, Direct Wavelength-Selective Optical and Electron-Beam Lithography of Functional Inorganic Nanomaterials, *ACS Nano*, 2019, **13**, 13917–13931.
15 M. Baláž, A. Zorkovská, F. Urakaev, P. Baláž, J. Briančin, Z. Bujňáková, M. Achimovičová and E. Gock, Ultrafast mechanochemical synthesis of copper sulfides, *RSC Adv.*, 2016, **6**, 87836–87842.
16 Y. Li, F. Huang, Q. Zhang and Z. Gu, Solvothermal synthesis of nanocrystalline cadmium sulfide, *J. Mater. Sci.*, 2000, **35**, 5933–5937.
17 G. Fu, L. Ding, Y. Chen, J. Lin, Y. Tang and T. Lu, Facile water-based synthesis and catalytic properties of platinum–gold alloy nanocubes, *CrystEngComm*, 2014, **16**, 1606–1610.
18 J. Zhang, R. W. Crisp, J. Gao, D. M. Kroupa, M. C. Beard and J. M. Luther, Synthetic Conditions for High-Accuracy Size Control of PbS Quantum Dots, *J. Phys. Chem. Lett.*, 2015, **6**, 1830–1833.
19 J. Zhu and M. C. Hersam, Assembly and Electronic Applications of Colloidal Nanomaterials, *Adv. Mater.*, 2017, **29**, 1603895.
20 M. Zeng and Y. Zhang, Colloidal nanoparticle inks for printing functional devices: emerging trends and future prospects, *J. Mater. Chem. A*, 2019, **7**, 23301–23336.
21 B. Mason, *Principles of Geochemistry*, John Wiley and Sons, 2nd edn, 1952.
22 A. P. Vinogradov, Average Contents of Chemical Elements in the Major Types of Terrestrial Igneous Rocks, *Geokhimiya*, 1962, **7**, 555–571.
23 W. M. Haynes, *CRC handbook of chemistry and physics*, CRC press, Boca Raton, Lodon, New York, 95th edn, 2014.
24 K. H. Wedepohl, The Composition of the Continental Crust, *Geochim. Cosmochim. Acta*, 1995, **59**, 1217–1232.
25 R. Steudel and B. Eckert, in *Elemental Sulfur and Sulfur-Rich Compounds I*, ed. R. Steudel, Springer Berlin Heidelberg, Berlin, Heidelberg, 2003, pp. 1–80, DOI: 10.1007/b12110.
26 R. Steudel, Berlin, Heidelberg, 1982.
27 X. Zhong, S. Liu, Z. Zhang, L. Li, Z. Wei and W. Knoll, Synthesis of high-quality CdS, ZnS, and ZnxCd1 − xS nanocrystals using metal salts and elemental sulfur, *J. Mater. Chem.*, 2004, **14**, 2790–2794.
28 J. Joo, H. B. Na, T. Yu, J. H. Yu, Y. W. Kim, F. Wu, J. Z. Zhang and T. Hyeon, Generalized and Facile Synthesis of Semiconducting Metal Sulfide Nanocrystals, *J. Am. Chem. Soc.*, 2003, **125**, 11100–11105.
29 J. H. Yu, J. Joo, H. M. Park, S.-I. Baik, Y. W. Kim, S. C. Kim and T. Hyeon, Synthesis of Quantum-Sized Cubic ZnS Nanorods by the Oriented Attachment Mechanism, *J. Am. Chem. Soc.*, 2005, **127**, 5662–5670.
30 D. Moodelly, P. Kowalik, P. Bujak, A. Pron and P. Reiss, Synthesis, photophysical properties and surface chemistry of chalcopyrite-type semiconductor nanocrystals, *J. Mater. Chem. C*, 2019, **7**, 11665–11709.
31 R. E. Davis and H. F. Nakshbendi, Sulfur in Amine Solvents, *J. Am. Chem. Soc.*, 1962, **84**, 2085–2090.
32 J. Ouyang, Photoluminescent Colloidal CdS Nanocrystals with High Quality via Noninjection One-Pot Synthesis in 1-Octadecene, *J. Phys. Chem. C*, 2009, 7579–7593.
33 M. Gao, H. Yang, H. Shen, Z. Zeng, F. Fan, B. Tang, J. Min, Y. Zhang, Q. Hua, L. S. Li, B. Ji and Z. Du, Bulk-like ZnSe Quantum Dots Enabling Efficient Ultranarrow Blue Light-Emitting Diodes, *Nano Lett.*, 2021, **21**, 7252–7260.
34 V. Mauritz, K. E. Dehm, S. P. Hager and R. W. Crisp, Colloidal nanocrystal synthesis of alkaline earth metal sulfides for solution-processed solar cell contact layers, *Z. Kristallogr. – Cryst. Mater.*, 2023, **238**, 295–300.
35 J. W. Thomson, K. Nagashima, P. M. Macdonald and G. A. Ozin, From sulfur-amine solutions to metal sulfide nanocrystals: peering into the oleylamine-sulfur black box, *J. Am. Chem. Soc.*, 2011, **133**, 5036–5041.
36 S. Ashoka Sahadevan, X. Xiao, Y. Ma, K. Forsberg, R. T. Olsson and J. M. Gardner, Sulfur–oleylamine copolymer synthesized via inverse vulcanization for the selective recovery of copper from lithium-ion battery E-waste, *Mater. Chem. Front.*, 2023, **7**, 1374–1384.
37 N. P. Tarasova, A. A. Zanin, E. G. Krivoborodov and Y. O. Mezhuev, Elemental sulphur in the synthesis of sulphur-containing polymers: reaction mechanisms and green prospects, *RSC Adv.*, 2021, **11**, 9008–9020.
38 W. J. Chung, J. J. Griebel, E. T. Kim, H. Yoon, A. G. Simmonds, H. J. Ji, P. T. Dirlam, R. S. Glass, J. J. Wie, N. A. Nguyen, B. W. Guralnick, J. Park, A. Somogyi, P. Theato, M. E. Mackay, Y. E. Sung, K. Char and J. Pyun, The use of elemental sulfur as an alternative feedstock for polymeric materials, *Nat. Chem.*, 2013, **5**, 518–524.
39 T. R. Martin, K. A. Mazzio, H. W. Hillhouse and C. K. Luscombe, Sulfur copolymer for the direct synthesis of ligand-free CdS nanoparticles, *Chem. Commun.*, 2015, **51**, 11244–11247.
40 J. H. L. Beal, P. G. Etchegoin and R. D. Tilley, Transition Metal Polysulfide Complexes as Single-Source Precursors for Metal Sulfide Nanocrystals, *J. Phys. Chem. C*, 2010, **114**, 3817–3821.
41 Z. Li, Y. Ji, R. Xie, S. Y. Grisham and X. Peng, Correlation of CdS Nanocrystal Formation with Elemental Sulfur Activation and Its Implication in Synthetic Development, *J. Am. Chem. Soc.*, 2011, **133**, 17248–17256.
42 H. Yu, Y. Liu and S. L. Brock, Synthesis of Discrete and Dispersible MoS_2 Nanocrystals, *Inorg. Chem.*, 2008, **47**, 1428–1434.
43 M. Protière and P. Reiss, Facile synthesis of monodisperse ZnS capped CdS nanocrystals exhibiting efficient blue emission, *Nanoscale Res. Lett.*, 2006, **1**, 62.
44 B. Meyer, Elemental sulfur, *Chem. Rev.*, 1976, **76**, 367–388.
45 W. A. Pryor, *Mechanisms of Sulfur Reactions*, McGraw-Hill, 1962.
46 M. R. McPhail and E. A. Weiss, Role of Organosulfur Compounds in the Growth and Final Surface Chemistry of PbS Quantum Dots, *Chem. Mater.*, 2014, **26**, 3377–3384.
47 C. G. Moore and J. Scanlan, Determination of Degree of Crosslinking in Natural Rubber Vulcanizates. Part VI.

Evidence for Chain Scission during the Crosslinking of Natural Rubber with Organic Peroxides, *Rubber Chem. Technol.*, 1961, **34**, 309–317.

48 M. G. Panthani, V. Akhavan, B. Goodfellow, J. P. Schmidtke, L. Dunn, A. Dodabalapur, P. F. Barbara and B. A. Korgel, Synthesis of $CuInS_2$, $CuInSe_2$, and $Cu(InxGa_{1-x})Se_2$ (CIGS) Nanocrystal "Inks" for Printable Photovoltaics, *J. Am. Chem. Soc.*, 2008, **130**, 16770–16777.

49 F. Jiang, L. T. Peckler and A. J. Muscat, Phase Pure Pyrite FeS_2 Nanocubes Synthesized Using Oleylamine as Ligand, Solvent, and Reductant, *Cryst. Growth Des.*, 2015, **15**, 3565–3572.

50 Y. Li, E. C. Y. Liu, N. Pickett, P. J. Skabara, S. S. Cummins, S. Ryley, A. J. Sutherland and P. O'Brien, Synthesis and characterization of CdS quantum dots in polystyrene microbeads, *J. Mater. Chem.*, 2005, **15**, 1238–1243.

51 A. Puglisi, S. Mondini, S. Cenedese, A. M. Ferretti, N. Santo and A. Ponti, Monodisperse Octahedral α-MnS and MnO Nanoparticles by the Decomposition of Manganese Oleate in the Presence of Sulfur, *Chem. Mater.*, 2010, **22**, 2804–2813.

52 E. Dilena, Y. Xie, R. Brescia, M. Prato, L. Maserati, R. Krahne, A. Paolella, G. Bertoni, M. Povia, I. Moreels and L. Manna, $CuInxGa_{1-x}S_2$ Nanocrystals with Tunable Composition and Band Gap Synthesized via a Phosphine-Free and Scalable Procedure, *Chem. Mater.*, 2013, **25**, 3180–3187.

53 J. Ning, K. Men, G. Xiao, L. Wang, Q. Dai, B. Zou, B. Liu and G. Zou, Facile synthesis of iv-vi SnS nanocrystals with shape and size control: nanoparticles, nanoflowers and amorphous nanosheets, *Nanoscale*, 2010, **2**, 1699–1703.

54 J. Ning, S. V. Kershaw and A. L. Rogach, Synthesis and Optical Properties of Cubic Chalcopyrite/Hexagonal Wurtzite Core/Shell Copper Indium Sulfide Nanocrystals, *J. Am. Chem. Soc.*, 2019, **141**, 20516–20524.

55 P. Li, L. Wang, L. Wang and Y. Li, Controlled synthesis and luminescence of semiconductor nanorods, *Chemistry*, 2008, **14**, 5951–5956.

56 E. P. Agency, Report on Carcinogens, **https://ntp.niehs.nih.gov/sites/default/files/ntp/roc/content/profiles/thioacetamide.pdf**.

57 R. T. Sanderson, Electronegativity and Bond Energy, *J. Am. Chem. Soc.*, 1983, **105**, 2259–2261.

58 G. Opitz, Sulfines and Sulfenes – the S-Oxides and S,S-Dioxides of Thioaldehydes and Thioketones, *Angew. Chem., Int. Ed. Engl.*, 1967, **6**, 107–123.

59 S. Q. Sun and T. Li, Synthesis and Characterization of CdS Nanoparticles and Nanorods via Solvo-Hydrothermal Route, *Cryst. Growth Des.*, 2007, **7**, 2367–2371.

60 L. Zhang and L. Yang, Hydrothermal growth of ZnS microspheres and their temperature-dependent luminescence properties, *Cryst. Res. Technol.*, 2008, **43**, 1022–1025.

61 K. A. Petrov and L. N. Andreev, The Chemical Properties of Thioacetamide, *Russ. Chem. Rev.*, 1971, **40**, 505–524.

62 H. He, S. Mei, Z. Chen, S. Liu, Z. Wen, Z. Cui, D. Yang, W. Zhang, F. Xie, B. Yang, R. Guo and G. Xing, Thioacetamide-ligand-mediated synthesis of CsPbBr3–CsPbBr3 homostructured nanocrystals with enhanced stability, *J. Mater. Chem. C*, 2021, **9**, 11349–11357.

63 C. Behera, R. Samal, C. S. Rout, R. S. Dhaka, G. Sahoo and S. L. Samal, Synthesis of $CuSbS_{(2)}$ Nanoplates and $CuSbS_{(2)}$-$Cu_{(3)}SbS_{(4)}$ Nanocomposite: Effect of Sulfur Source on Different Phase Formation, *Inorg. Chem.*, 2019, **58**, 15291–15302.

64 T. J. Huang, X. Yin, C. Tang, G. Qi and H. Gong, A low-cost, ligand exchange-free strategy to synthesize large-grained Cu_2ZnSnS_4 thin-films without a fine-grain underlayer from nanocrystals, *J. Mater. Chem. A*, 2015, **3**, 17788–17796.

65 T. Wu, X. Zhou, H. Zhang and X. Zhong, Bi_2S_3 nanostructures: A new photocatalyst, *Nano Res.*, 2010, **3**, 379–386.

66 P. An, Z. Liang, X. Xu, X. Wang, H. Jin, N. Wang, J. Wang and F. Zhu, A heating-up method for the synthesis of pure phase kesterite Cu_2ZnSnS_4nanocrystals using a simple coordinating sulphur precursor, *RSC Adv.*, 2015, **5**, 6879–6885.

67 M. Tamilselvan and A. J. Bhattacharyya, Tetrahedrite (Cu12Sb4S13) Ternary Inorganic Hole Conductor for Ambient Processed Stable Perovskite Solar Cells, *ACS Appl. Energy Mater.*, 2018, **1**, 4227–4234.

68 B. Ni, T. He, J. O. Wang, S. Zhang, C. Ouyang, Y. Long, J. Zhuang and X. Wang, The formation of $(NiFe)S_{(2)}$ pyrite mesocrystals as efficient pre-catalysts for water oxidation, *Chem. Sci.*, 2018, **9**, 2762–2767.

69 A. Méndez-López, A. Morales-Acevedo, Y. D. J. Acosta-Silva, H. Katagiri, Y. Matsumoto, O. Zelaya-Angel and M. Ortega-López, Study of the synthesis of self- assembled tin disulfide nanoparticles prepared by a low-cost process, *Phys. Status Solidi C*, 2015, **12**, 564–567.

70 W. C. Huang, C. H. Tseng, S. H. Chang, H. Y. Tuan, C. C. Chiang, L. M. Lyu and M. H. Huang, Solvothermal synthesis of zincblende and wurtzite $CuInS_2$ nanocrystals and their photovoltaic application, *Langmuir*, 2012, **28**, 8496–8501.

71 H. J. Lee, S. Im, D. Jung, K. Kim, J. A. Chae, J. Lim, J. W. Park, D. Shin, K. Char, B. G. Jeong, J.-S. Park, E. Hwang, D. C. Lee, Y.-S. Park, H.-J. Song, J. H. Chang and W. K. Bae, Coherent heteroepitaxial growth of I-III-VI_2 $Ag(In,Ga)S_2$ colloidal nanocrystals with near-unity quantum yield for use in luminescent solar concentrators, *Nat. Commun.*, 2023, **14**, 3779.

72 H. O. Pritchard and H. A. Skinner, The concept of electronegativity, *Chem. Rev.*, 1955, **55**, 745–786.

73 R. G. Pearson, Hard and soft acids and bases, *J. Am. Chem. Soc.*, 1963, **85**, 3533–3539.

74 X. Lu, Z. Zhuang, Q. Peng and Y. Li, Controlled synthesis of wurtzite $CuInS_2$ nanocrystals and their side-by-side nanorod assemblies, *CrystEngComm*, 2011, **13**, 4039–4045.

75 A. Singh, H. Geaney, F. Laffir and K. M. Ryan, Colloidal synthesis of wurtzite Cu_2ZnSnS_4 nanorods and their perpendicular assembly, *J. Am. Chem. Soc.*, 2012, **134**, 2910–2913.

76 Q. Liu, A. Diaz, A. Prosvirin, Z. Luo and J. D. Batteas, Shape-controlled synthesis of nanopyramids and nanoprisms of nickel sulfide (Ni_3S_4), *Nanoscale*, 2014, **6**, 8935–8942.

77 L. Chen, H. Hu, Y. Chen, Y. Li, J. Gao and G. Li, Sulfur Precursor Reactivity Affecting the Crystal Phase and Morphology of $Cu_{(2-x)}S$ Nanoparticles, *Chemistry*, 2021, **27**, 1057–1065.

78 K. E. Dehm, A. Zanetti, B. Fett, V. Mauritz, R. C. Hamburger, D. Langford, D. M. Guldi, E. R. Young, K. Mandel and R. W. Crisp, Alteration of the Optoelectronic Properties of $CuInS_2$ Quantum Dots via Colloidal Annealing, *Cryst. Growth Des.*, 2024, **24**, 4131–4135.
79 J. Heo, G. H. Kim, J. Jeong, Y. J. Yoon, J. H. Seo, B. Walker and J. Y. Kim, Clean thermal decomposition of tertiary-alkyl metal thiolates to metal sulfides: environmentally-benign, non-polar inks for solution-processed chalcopyrite solar cells, *Sci. Rep.*, 2016, **6**, 36608.
80 D. A. D. E. V. Anslyn, *Moder Physical Organic Chemistry*, 2000.
81 C. Imla Mary, M. Senthilkumar and S. Moorthy Babu, Influence of different sulfur sources on the phase formation of Cu_2ZnSnS_4 (CZTS) nanoparticles (NPs), *J. Mater. Sci.: Mater. Electron.*, 2018, **29**, 9751–9756.
82 W. Zhang and X. Zhong, Facile Synthesis of ZnS−$CuInS_2$-Alloyed Nanocrystals for a Color-Tunable Fluorchrome and Photocatalyst, *Inorg. Chem.*, 2011, **50**, 4065–4072.
83 V. Grigel, D. Dupont, K. De Nolf, Z. Hens and M. D. Tessier, InAs Colloidal Quantum Dots Synthesis via Aminopnictogen Precursor Chemistry, *J. Am. Chem. Soc.*, 2016, **138**, 13485–13488.
84 M. D. Tessier, K. De Nolf, D. Dupont, D. Sinnaeve, J. De Roo and Z. Hens, Aminophosphines: A Double Role in the Synthesis of Colloidal Indium Phosphide Quantum Dots, *J. Am. Chem. Soc.*, 2016, **138**, 5923–5929.
85 R. W. Crisp, G. Grimaldi, L. De Trizio, W. Evers, N. Kirkwood, S. Kinge, L. Manna, L. Siebbeles and A. J. Houtepen, Selective antimony reduction initiating the nucleation and growth of InSb quantum dots, *Nanoscale*, 2018, **10**, 11110–11116.
86 P. Nørby, S. Johnsen and B. B. Iversen, *In Situ* X-ray Diffraction Study of the Formation, Growth, and Phase Transition of Colloidal $Cu_{2-x}S$ Nanocrystals, *ACS Nano*, 2014, **8**, 4295–4303.
87 W. van der Stam, F. T. Rabouw, J. J. Geuchies, A. C. Berends, S. O. M. Hinterding, R. G. Geitenbeek, J. van der Lit, S. Prévost, A. V. Petukhov and C. de Mello Donega, In Situ Probing of Stack-Templated Growth of Ultrathin $Cu_{2-x}S$ Nanosheets, *Chem. Mater.*, 2016, **28**, 6381–6389.
88 A. S. R. Chesman, N. W. Duffy, S. Peacock, L. Waddington, N. A. S. Webster and J. J. Jasieniak, Non-injection synthesis of Cu_2ZnSnS_4 nanocrystals using a binary precursor and ligand approach, *RSC Adv.*, 2013, **3**, 1017–1020.
89 J. M. Rhodes, C. A. Jones, L. B. Thal and J. E. Macdonald, Phase-Controlled Colloidal Syntheses of Iron Sulfide Nanocrystals via Sulfur Precursor Reactivity and Direct Pyrite Precipitation, *Chem. Mater.*, 2017, **29**, 8521–8530.
90 M. J. Turo and J. E. Macdonald, Crystal-Bound vs Surface-Bound Thiols on Nanocrystals, *ACS Nano*, 2014, **8**, 10205–10213.
91 M. L. H. Green and G. Parkin, Application of the Covalent Bond Classification Method for the Teaching of Inorganic Chemistry, *J. Chem. Educ.*, 2014, **91**, 807–816.
92 S. Kern, G. Yi, P. Büttner, F. Scheler, M.-H. Tran, S. Korenko, K. E. Dehm, I. Kundrata, A. Zahl, S. Albrecht, J. Bachmann and R. W. Crisp, Monolithic Two-Terminal Tandem Solar Cells Using Sb_2S_3 and Solution-Processed PbS Quantum Dots Achieving an Open-Circuit Potential beyond 1.1 V, *ACS Appl. Mater. Interfaces*, 2024, **16**, 13903–13913.
93 M. Li, J. Ouyang, C. I. Ratcliffe, L. Pietri, X. Wu, D. M. Leek, I. Moudrakovski, Q. Lin, B. Yang and K. Yu, CdS Magic-Sized Nanocrystals Exhibiting Bright Band Gap Photoemission via Thermodynamically Driven Formation, *ACS Nano*, 2009, **3**, 3832–3838.
94 K. V. Kravchyk, M. V. Kovalenko and M. I. Bodnarchuk, Colloidal Antimony Sulfide Nanoparticles as a High-Performance Anode Material for Li-ion and Na-ion Batteries, *Sci. Rep.*, 2020, **10**, 2554.
95 C. C. Reinhart and E. Johansson, Colloidally Prepared 3-Mercaptopropionic Acid Capped Lead Sulfide Quantum Dots, *Chem. Mater.*, 2015, **27**, 7313–7320.
96 C. Chatgilialoglu, C. Ferreri, Y. Landais and V. I. Timokhin, Thirty Years of (TMS)3SiH: A Milestone in Radical-Based Synthetic Chemistry, *Chem. Rev.*, 2018, **118**, 6516–6572.
97 D. So and G. Konstantatos, Thiol-Free Synthesized Copper Indium Sulfide Nanocrystals as Optoelectronic Quantum Dot Solids, *Chem. Mater.*, 2015, **27**, 8424–8432.
98 L. Truong, I. S. Moody, D. P. Stankus, J. A. Nason, M. C. Lonergan and R. L. Tanguay, Differential stability of lead sulfide nanoparticles influences biological responses in embryonic zebrafish, *Arch. Toxicol.*, 2011, **85**, 787–798.
99 M. A. Hines and G. D. Scholes, Colloidal PbS Nanocrystals with Size-Tunable Near-Infrared Emission: Observation of Post-Synthesis Self-Narrowing of the Particle Size Distribution, *Adv. Mater.*, 2003, **15**, 1844–1849.
100 C. B. Murray, D. J. Norris and M. G. Bawendi, Synthesis and characterization of nearly monodisperse CdE (E = sulfur, selenium, tellurium) semiconductor nanocrystallites, *J. Am. Chem. Soc.*, 1993, **115**, 8706–8715.
101 H. Fu, S.-W. Tsang, Y. Zhang, J. Ouyang, J. Lu, K. Yu and Y. Tao, Impact of the Growth Conditions of Colloidal PbS Nanocrystals on Photovoltaic Device Performance, *Chem. Mater.*, 2011, **23**, 1805–1810.
102 P. Glaser, O. Stewart Jr., R. Atif, D. R. C. Asuigui, J. Swanson, A. J. Biacchi, A. R. Hight Walker, G. Morrison, H.-C. zur Loye and S. L. Stoll, Synthesis of Mixed-Valent Lanthanide Sulfide Nanoparticles, *Angew. Chem., Int. Ed.*, 2021, **60**, 23134–23141.
103 Y. Zhang, T. D. Siegler, C. J. Thomas, M. K. Abney, T. Shah, A. De Gorostiza, R. M. Greene and B. A. Korgel, A "Tips and Tricks" Practical Guide to the Synthesis of Metal Halide Perovskite Nanocrystals, *Chem. Mater.*, 2020, **32**, 5410–5423.
104 A. Antanovich, A. Prudnikau and M. Artemyev, Formation of Ultrasmall PbS Nanocrystals in Octadecene at Mild Temperature Promoted by Alcohol or Acetone Injection, The, *J. Phys. Chem. C*, 2014, **118**, 21104–21109.
105 P. J. Heard, *Progress in Inorganic Chemistry*, John Wiley & Sons, 2005.
106 M. K. Amir, R. Ziaur, F. Hayat, S. Z. Khan, G. Hogarth, T. Kondratyuk, J. M. Pezzuto and M. N. Tahir, Monofunctional platinum(II) dithiocarbamate complexes: synthesis, characterization and anticancer activity, *RSC Adv.*, 2016, **6**, 110517–110524.

107 G. Hogarth, *Progress in Inorganic Chemistry*, 2005, 71–561, DOI: 10.1002/0471725587.ch2.
108 A. Roffey, N. Hollingsworth and G. Hogarth, Synthesis of ternary sulfide nanomaterials using dithiocarbamate complexes as single source precursors, *Nanoscale Adv.*, 2019, **1**, 3056–3066.
109 H. Jiang, P. Dai, Z. Feng, W. Fan and J. Zhan, Phase selective synthesis of metastable orthorhombic Cu_2ZnSnS_4, *J. Mater. Chem.*, 2012, **22**, 7502–7506.
110 H. U. Islam, A. Roffey, N. Hollingsworth, W. Bras, G. Sankar, N. H. De Leeuw and G. Hogarth, Understanding the role of zinc dithiocarbamate complexes as single source precursors to ZnS nanomaterials, *Nanoscale Adv.*, 2020, **2**, 798–807.
111 N. Hollingsworth, A. Roffey, H.-U. Islam, M. Mercy, A. Roldan, W. Bras, M. Wolthers, C. R. A. Catlow, G. Sankar, G. Hogarth and N. H. de Leeuw, Active Nature of Primary Amines during Thermal Decomposition of Nickel Dithiocarbamates to Nickel Sulfide Nanoparticles, *Chem. Mater.*, 2014, **26**, 6281–6292.
112 A. Roffey, N. Hollingsworth, H.-U. Islam, W. Bras, G. Sankar, N. H. de Leeuw and G. Hogarth, Fe(II) and Fe(III) dithiocarbamate complexes as single source precursors to nanoscale iron sulfides: a combined synthetic and in situ XAS approach, *Nanoscale Adv.*, 2019, **1**, 2965–2978.
113 F. S. Bourier, Effect of Residual Water on the Nucleation and Growth of Gold Nanoparticles in an Amine-mediated Synthesis in Organic Solvents, PhD thesis, University of Hamburg, 2022.
114 H.-U. Islam, A. Roffey, N. Hollingsworth, W. Bras, G. Sankar, N. H. De Leeuw and G. Hogarth, Understanding the role of zinc dithiocarbamate complexes as single source precursors to ZnS nanomaterials, *Nanoscale Adv.*, 2020, **2**, 798–807.
115 L. D. Nyamen, N. Revaprasadu, R. V. S. R. Pullabhotla, A. A. Nejo, P. T. Ndifon, M. A. Malik and P. O'Brien, Synthesis of multi-podal CdS nanostructures using heterocyclic dithiocarbamato complexes as precursors, *Polyhedron*, 2013, **56**, 62–70.
116 G. A. Tigwere, M. D. Khan, L. D. Nyamen, A. A. Aboud, T. Moyo, S. T. Dlamini, P. T. Ndifon and N. Revaprasadu, Molecular precursor route for the phase selective synthesis of α-MnS or metastable γ-MnS nanomaterials for magnetic studies and deposition of thin films by AACVD, *Mater. Sci. Semicond. Process.*, 2022, **139**, 106330.
117 A. Dirksen, P. J. Nieuwenhuizen, M. Hoogenraad, J. G. Haasnoot and J. Reedijk, New mechanism for the reaction of amines with zinc dithiocarbamates, *J. Appl. Polym. Sci.*, 2001, **79**, 1074–1083.
118 X.-Y. Chen, J. Li and C.-S. Jia, Thermodynamic Properties of Gaseous Carbon Disulfide, *ACS Omega*, 2019, **4**, 16121–16124.
119 R. O. Beauchamp, J. S. Bus, J. A. Popp, C. J. Boreiko, L. Goldberg and M. J. McKenna, A Critical Review of the Literature on Carbon Disulfide Toxicity, *CRC Crit. Rev. Toxicol.*, 1983, **11**, 169–278.
120 R. Ahmad, N. U. Saddiqi, M. Wu, M. Prato, E. Spiecker, W. Peukert and M. Distaso, Effect of the Counteranion on the Formation Pathway of $Cu_{(2)}ZnSnS_{(4)}$ (CZTS) Nanoparticles under Solvothermal Conditions, *Inorg. Chem.*, 2020, **59**, 1973–1984.
121 M. Ballabeni, R. Ballini, F. Bigi, R. Maggi, M. Parrini, G. Predieri and G. Sartori, Synthesis of Symmetrical *N*,*N*′-Disubstituted Thioureas and Heterocyclic Thiones from Amines and $CS_{(2)}$ over a $ZnO/Al_{(2)}O_{(3)}$ Composite as Heterogeneous and Reusable Catalyst, *J. Org. Chem.*, 1999, **64**, 1029–1032.
122 G. Barim, S. R. Smock, P. D. Antunez, D. Glaser and R. L. Brutchey, Phase control in the colloidal synthesis of well-defined nickel sulfide nanocrystals, *Nanoscale*, 2018, **10**, 16298–16306.
123 E. Bennett, M. W. Greenberg, A. J. Jordan, L. S. Hamachi, S. Banerjee, S. J. L. Billinge and J. S. Owen, Size Dependent Optical Properties and Structure of ZnS Nanocrystals Prepared from a Library of Thioureas, *Chem. Mater.*, 2022, **34**, 706–717.
124 Y. Vahidshad, M. N. Tahir, A. I. zad, S. M. Mirkazemi, R. Ghazemzadeh and W. Tremel, Structural and optical properties of Fe and Zn substituted $CuInS_2$ nanoparticles synthesized by a one-pot facile method, *J. Mater. Chem. C*, 2015, **3**, 889–898.
125 M. P. Hendricks, M. P. Campos, G. T. Cleveland, I. Jen-La Plante and J. S. Owen, A tunable library of substituted thiourea precursors to metal sulfide nanocrystals, *Science*, 2015, **348**, 1226–1230.
126 G. A. Bowmaker, J. V. Hanna, C. Pakawatchai, B. W. Skelton, Y. Thanyasirikul and A. H. White, Crystal Structures and Vibrational Spectroscopy of Copper(I) Thiourea Complexes, *Inorg. Chem.*, 2009, **48**, 350–368.
127 S. Rakhshani, A. R. Rezvani, M. Dusek and V. Eigner, Design and fabrication of novel thiourea coordination compounds as potent inhibitors of bacterial growth, *J. Antibiot.*, 2019, **72**, 260–270.
128 A. A. Shults, G. Lu, J. D. Caldwell and J. E. Macdonald, Role of carboxylates in the phase determination of metal sulfide nanoparticles, *Nanoscale Horiz.*, 2023, **8**, 1386–1394.
129 F. Manteiga Vázquez, Q. Yu, L. F. Klepzig, L. D. A. Siebbeles, R. W. Crisp and J. Lauth, Probing Excitons in Ultrathin PbS Nanoplatelets with Enhanced Near-Infrared Emission, *J. Phys. Chem. Lett.*, 2021, **12**, 680–685.
130 K.-D. Wehrstedt, W. Wildner, T. Güthner, K. Holzrichter, B. Mertschenk and A. Ulrich, Safe transport of cyanamide, *J. Hazard. Mater.*, 2009, **170**, 829–835.
131 D. C. Schröder, *Thioureas*, American Chemical Society, 1954.
132 Z. Jia, Y. Dai, H. Shao, J. Xu, Q. Meng and J. Qiao, Room-Temperature, Multigram-Scale Synthesis and Conversion Mechanism of Highly Luminescent Lead Sulfide Quantum Dots, *J. Phys. Chem. Lett.*, 2023, **14**, 8129–8137.
133 A. K. M. a R. Ashare, *Isothiocyanat in the Chemistry of Heterocycles*, American Chemical Society, 1991, vol. 91.
134 L. Loghina, M. Grinco, A. Iakovleva, S. Slang, K. Palka and M. Vlcek, Mechanistic investigation of the sulfur precursor evolution in the synthesis of highly photoluminescent $Cd_{0.15}Zn_{0.85}S$ quantum dots, *New J. Chem.*, 2018, **42**, 14779–14788.

135 T. P. A. Ruberu, H. R. Albright, B. Callis, B. Ward, J. Cisneros, H.-J. Fan and J. Vela, Molecular Control of the Nanoscale: Effect of Phosphine–Chalcogenide Reactivity on CdS–CdSe Nanocrystal Composition and Morphology, *ACS Nano*, 2012, **6**, 5348–5359.

136 D. V. Talapin, J. H. Nelson, E. V. Shevchenko, S. Aloni, B. Sadtler and A. P. Alivisatos, Seeded Growth of Highly Luminescent CdSe/CdS Nanoheterostructures with Rod and Tetrapod Morphologies, *Nano Lett.*, 2007, **7**, 2951–2959.

137 M. Lazell and P. O'Brien, Synthesis of CdS nanocrystals using cadmium dichloride and trioctylphosphine sulfide, *J. Mater. Chem.*, 1999, **9**, 1381–1382.

138 H. Liu, J. S. Owen and A. P. Alivisatos, Mechanistic Study of Precursor Evolution in Colloidal Group II–VI Semiconductor Nanocrystal Synthesis, *J. Am. Chem. Soc.*, 2007, **129**, 305–312.

139 R. Mahadevu, H. Kaur and A. Pandey, Hidden role of anion exchange reactions in nucleation of colloidal nanocrystals, *CrystEngComm*, 2016, **18**, 759–764.

140 F. Fan, O. Voznyy, R. P. Sabatini, K. T. Bicanic, M. M. Adachi, J. R. McBride, K. R. Reid, Y.-S. Park, X. Li, A. Jain, R. Quintero-Bermudez, M. Saravanapavanantham, M. Liu, M. Korkusinski, P. Hawrylak, V. I. Klimov, S. J. Rosenthal, S. Hoogland and E. H. Sargent, Continuous-wave lasing in colloidal quantum dot solids enabled by facet-selective epitaxy, *Nature*, 2017, **544**, 75–79.

141 F. Jamal, A. Rafique, S. Moeen, J. Haider, W. Nabgan, A. Haider, M. Imran, G. Nazir, M. Alhassan, M. Ikram, Q. Khan, G. Ali, M. Khan, W. Ahmad and M. Maqbool, Review of Metal Sulfide Nanostructures and their Applications, *ACS Appl. Nano Mater.*, 2023, **6**, 7077–7106.

142 K. V. Sopiha, C. Comparotto, J. A. Márquez and J. J. S. Scragg, Chalcogenide Perovskites: Tantalizing Prospects, Challenging Materials, *Adv. Opt. Mater.*, 2021, **10**, 2101704.

143 A. Pein, M. Baghbanzadeh, T. Rath, W. Haas, E. Maier, H. Amenitsch, F. Hofer, C. O. Kappe and G. Trimmel, Investigation of the Formation of $CuInS_2$ Nanoparticles by the Oleylamine Route: Comparison of Microwave-Assisted and Conventional Syntheses, *Inorg. Chem.*, 2011, **50**, 193–200.

144 D. Zilevu and S. E. Creutz, Shape-Controlled Synthesis of Colloidal Nanorods and Nanoparticles of Barium Titanium Sulfide, *Chem. Mater.*, 2021, **33**, 5137–5146.

